Molecular Vision 2020; 26:679-690 <http://www.molvis.org/molvis/v26/679>
Received 3 February 2020 | Accepted 8 October 2020 | Published 10 October 2020

Ablation of C3 modulates macrophage reactivity in the outer retina during photo-oxidative damage

Haihan Jiao,[1,2] Jan M. Provis,[2,3] Riccardo Natoli,[2,3] Matt Rutar[4]

(The last two authors are co-senior authors for this study.)

[1]Department of Optometry and Vision Science, University of Melbourne, Victoria, Australia; [2]The John Curtin School of Medical Research, The Australian National University, Acton, Australia; [3]The Australian National University Medical School, Acton, Australia; [4]Department of Anatomy and Neuroscience, University of Melbourne, Victoria, Australia

Purpose: Dysregulation of the complement cascade contributes to a variety of retinal dystrophies, including age-related macular degeneration (AMD). The central component of complement, C3, is expressed in abundance by macrophages in the outer retina, and its ablation suppresses photoreceptor death in experimental photo-oxidative damage. Whether this also influences macrophage reactivity in this model system, however, is unknown. We investigate the effect of C3 ablation on macrophage activity and phagocytosis by outer retinal macrophages during photo-oxidative damage.
Methods: Age-matched C3 knockout (KO) mice and wild-type (WT) C57/Bl6 mice were subjected to photo-oxidative damage. Measurements of the outer nuclear layer (ONL) thickness and terminal deoxynucleotidyl transferase dUTP nick end labeling (TUNEL) staining were used to assess pathology and photoreceptor apoptosis, respectively. Macrophage abundance and phagocytosis were assessed with immunolabeling for pan-macrophage and phagocytic markers, in conjunction with TUNEL staining in cohorts of C3 KO and WT mice.
Results: The C3 KO mice exhibited protection against photoreceptor cell death following photo-oxidative damage, which was associated with a reduction in immunoreactivity for the stress-related factor GFAP. In conjunction, there was a reduction in IBA1-positive macrophages in the outer retina compared to the WT mice and a decrease in the number of CD68-positive cells in the outer nuclear layer and the subretinal space. In addition, the engulfment of TUNEL-positive and -negative photoreceptors by macrophages was significantly lower in the C3 KO mice cohort following photo-oxidative damage compared to the WT cohort.
Conclusions: The results show that the absence of C3 mitigates the phagocytosis of photoreceptors by macrophages in the outer retina, and the net impact of C3 depletion is neuroprotective in the context of photo-oxidative damage. These data improve our understanding of the impact of C3 inhibition in subretinal inflammation and inform the development of treatments for targeting complement activation in diseases such as AMD.

The activation of an immune cascade known as the complement system is a crucial factor in the etiology of age-related macular degeneration (AMD). Complement contributes to a major arm of the innate immune response and provides a rapid response to a range of immunological challenges [1,2]. Three activating pathways comprise the complement cascade (classical, mannose-binding lectin, and alternative), and all converge on the proteolytic cleavage of C3 to generate an arsenal of inflammatory mediators, including the opsonin C3b and the anaphylatoxin C3a. This process is mediated chiefly by C3-convertases that are assembled from complement constituents such as C2, C4, CFB, and CFD in the presence of noxious stimuli. If left to propagate, the accumulation of C3b triggers cleavage of C5 to produce C5a and C5b, with the latter inducing the assembly of a membrane attack complex (MAC) that binds to cell surfaces, forming transmembrane channels that cause cytolysis or apoptosis of the target cells.

Polymorphisms in complement genes have been reported to account for approximately 70% of the risk for developing AMD, as demonstrated in multiple, independent genome-wide association studies (GWASs) [3,4]. The first reported strong associations between the Y402H polymorphism in complement factor H (CFH) with all forms of AMD, while later investigations also identified risk-conferring variants in other complement genes, including C3, C2, and CFB [3,4]. The current dogma of CFH function is to downregulate the complement cascade, by inhibiting cleavage of C3, limiting the generation of byproducts that spur inflammation. This feature prioritizes modifiers of C3 activation as potential therapeutics for ameliorating complement [5], although additional molecular studies are required to develop the groundwork needed for effective targeting of complement. Dysregulation of the cascade is also linked to a range of

Correspondence to: Haihan Jiao, University of Melbourne, Victoria, Australia 3052; Phone: +61390357545; email: helen.jiao@unimelb.edu.au

neurodegenerative conditions, including traumatic brain injury, Alzheimer disease, and Parkinson disease [6].

Complement expression and activation occur locally within the retina under pathological conditions with causative effects that are driven by a combination of genetic and environmental factors, such as photo-oxidative damage (PD) [7–9], smoking, and obesity [10], and leading to dysregulation of inflammatory cascades [11]. Over the last several years, several investigations have shown that macrophages are a source of complement components, particularly C3, and related regulatory factors [12,13]. These include rodent models of aging [14], obesity [15], PD [9,16,17], and most recently, retinitis pigmentosa [18]. The identification of retinal macrophages as a major source of C3 suggests that the abundance of these cells in the outer nuclear layer (ONL) and the subretinal space dictates the scale and duration of local complement activation that leads to cell death. The abundance of mononuclear phagocytes in the outer retina has been a feature of AMD [19,20] and occurs in several retinal degenerative animal models [19,21-24]. Our most recent study indicated that C3 is locally expressed by ONL and subretinal macrophages in postmortem tissues from patients with atrophic AMD, and that total ablation of C3 provides neuroprotection in PD [16]. This investigation and the previous report on mouse laser-induced choroidal neovascularization (CNV) [25] demonstrated that serum sources of complement are dispensable for inducing complement-mediated attack in PD and CNV, while local inhibition of C3 via RNA interference (RNAi) ameliorates complement deposition in the ONL and the subretinal space. A similar neuroprotective effect has since been observed in an experimental model of glaucoma [26].

Intriguingly, a recent study by Silverman and colleagues showed that total ablation of C3 suppresses photoreceptor death and that macrophages/microglia exhibit reduced phagocytosis of apoptotic photoreceptors [18]. The researchers' observations suggest that a degree of local complement expression may be necessary to facilitate apoptotic cell clearance and homeostasis, which is neuroprotective in instances where excessive and inappropriately regulated complement is not present. Recently, we showed that ablation of local C3 reduces photoreceptor death in the context of PD [16], although changes in the activity of reactive macrophages concerning the C3 ablation in this system are unknown. In the present study, we investigated the impact of C3 on macrophage morphology, abundance, and photoreceptor phagocytosis in the PD model and further explored the protective phenotype. The data show that macrophages of the outer retina (the ONL and the subretinal space) in C3 knockout (KO) mice exhibited a decrease in immunoreactivity for CD68 following PD. In addition, phagocytosis of terminal deoxynucleotidyl transferase dUTP nick end labeling (TUNEL)-positive and TUNEL-negative photoreceptors by macrophages was suppressed in the C3 KO mice after PD.

METHODS

Experimental animals: All experiments were conducted in accordance with the ARVO Statement for the Use of Animals in Ophthalmic and Vision Research and were approved by the Australian National University (ANU) Animal Experimentation Ethics Committee. Mice homozygous for C3 mutation, *C3*$^{-/-}$ mice (C3tm1Crr/J), and age-matched, isogenic wild-type (WT) littermates, bred on the C57BL/6J background, were used at 3 months of age. Both groups were subjected to PD following our established protocols [27], with food and water provided ad libitum. The mice were euthanized with cervical dislocation at either 1, 3, 5, or 7 days of PD.

TUNEL labeling of photoreceptor apoptosis: TUNEL was used to quantify photoreceptor apoptosis in retinal cryosections. The sections were permeabilized with 0.01 M PBS (1X; 120 mM NaCl, 20 mM KCl, 10 mM $NaPO_4$, 5 mM KPO_4, pH 7.4) and 0.1% Triton-X100 for 10 min at room temperature and then labeled using a TUNEL assay (Roche, Indianapolis, IN) according to the manufacturer's specifications. Counts of TUNEL-positive cells in the ONL were performed blind to the condition and genotype, and along the full-length of retinal cryosections cut along the vertical meridian (superior-inferior) including the optic disc. The final count for each animal was the average of those obtained at comparable locations in two retinal cryosections.

Immunohistochemical labeling of retinal sections: Retinal cryosections sections were used for immunohistochemical analysis. The primary antibodies are listed in Table 1. Some retinal sections were stained with TUNEL before immunohistochemistry. Cryosections were firstly subjected to heat-induced antigen retrieval using 100% Reveal-it (ImmunoSolution, QLD, Australia) for 1 h at 37 °C, then washed in 0.1 M PBS containing 0.3% Reveal-it, and blocked and permeabilized (10% normal goat serum in 1X PBS with 0.1% Triton X-100 for 1 h at room temperature). Following overnight incubation of the primary antibodies at 4 °C, the retinal sections were washed in 0.1 M PBS and then incubated with secondary antibodies: Alexa-488 conjugated goat anti-rabbit for IBA1 and GFAP, 4.0 h at room temperature and Streptavidin Alexa-594 conjugated anti-biotin for CD68, 1.5 h at room temperature (Thermo Fisher Scientific, NSW, Australia). The sections were then incubated with the DNA-specific dye bisbenzimide (1:10,000, Sigma-Aldrich, NSW,

Table 1. List of primary antibodies.

Antibody	Target	Source	Catalog #
Rabbit α-IBA1	Ionized calcium binding protein 1	Wako Chemicals (Osaka, Japan)	019–19741
Rat α-CD68/macrosialin	CD68:Biotin Clone FA-11	AbD Serotec (Hercules, CA)	MCA1957BT
Rabbit α-GFAP	Glial fibrillary acidic protein	Dako (Glostrup, Denmark)	Z0334

Australia) for 2 min, washed, and then coverslipped using Aqua-Poly/Mount (Polysciences, Warrington, PA).

Immunofluorescence in the retinal sections was visualized using a laser-scanning A1+ confocal microscope (Nikon, Tokyo, Japan), and images were acquired using the z-stack function of the NIS-Elements AR software (Nikon, Tokyo, Japan) under the same acquisition settings. Quantification analyses included retinal morphometric analysis and total counts of immunolabeled cells (GFAP, IBA, and CD68). Analyses were based on the average of two sections per experimental group of animals (n = 5–6 per group).

Quantification of GFAP immunofluorescence: The immunofluorescence intensity of GFAP and the length of immunolabeled GFAP-positive Müller glia were quantified in the confocal images of the WT and C3 KO mouse retinal sections. Confocal images of GFAP-labeled sections were processed and analyzed using the NIS-Elements AR software. Consistency in the analyses was ensured by employing identical parameters with areas sampled for the analysis, camera, and laser configuration. For each sample, an average of three consistent locations in the superior retina (500, 1,000, and 1,500 µm eccentricity) was used to account for geographic variability. The inferior retina was excluded because GFAP changes in this region were less pronounced for reliable quantification.

For quantification of fluorescence, the areas of interest were marked with a rectangle drawn from the apical surface of the ganglion cell layer (GCL) to the basal surface of the ONL, from which the mean fluorescent intensity for each retina was then collected. The mean GFAP fluorescent intensity was measured from each rectangle across the superior retina, and the average of two sections from each animal was taken (n = 5 per group). The length of the GFAP-positive Müller glia process was taken from within the lesion region of the superior retina, using selection tools from NIS-Elements AR software. The measurements were then averaged for each experimental group (n = 5 per group).

Quantification and analysis of outer retinal macrophages: The abundance and morphology of outer retinal macrophages in the WT and C3 KO mouse groups were quantified on retinal cryosections immunolabeled with IBA1 over the time course of PD (n = 5 per group). The amoeboid IBA1-positive macrophages were characterized by the circularity which is defined as perimeter^2 / area (P^2/A) and validated with the grid-cross analysis method. Higher circularity and a lower number of grid-crossed points per cell indicate a round cell, thus amoeboid morphology, whereas lower circularity indicates ramified morphology. The total number of ramified and amoeboid IBA1-positive cells was separately quantified in the outer retina (the ONL and the subretinal space) across the full length of the retinal cryosections in duplicate.

The phagocytic properties of outer retinal IBA1-positive macrophages following PD were assessed with quantification of immunolabeling for CD68 and their engulfment of photoreceptors. The total number of cells identified as IBA1-positive CD68-positive following immunolabeling on the retinal cryosections was quantified in the outer retina across the full length of the retinal cryosections (superior-inferior) after PD. The number of photoreceptor nuclei engulfed by outer retinal macrophages was determined using sections that were labeled for IBA1, TUNEL, and bisbenzamide. Counts were made of IBA1-positive cells in the ONL that had engulfed either TUNEL-positive or TUNEL-negative cells in each section. All counts were performed in six areas across the full length of the retina in duplicate (n = 6 per group).

For each quantitative confocal datum, the labels of the stained retinal cryosections were masked to collect and analyze the data in a blinded fashion. The data were quantified from an average of three consistent locations in the superior retina (500, 1,000, and 1,500 µm eccentricity), to account for geographic variability.

Retinal morphometric analysis: The retinal cryosections were stained with toluidine blue to assess changes in ONL integrity following PD and then quantified using an established methodology [27]. Briefly, the number of rows of photoreceptor nuclei was counted in six areas of the retinal cryosections (superior-inferior) from each group, the central, mid-periphery and peripheral retina, at 500 µm intervals across each section. In at least two retinal sections per animal, photoreceptor rows were counted per area and then averaged for each experimental group (n = 6 per group).

Statistical analyses: Statistical analyses were performed in Prism 7 (GraphPad Software, San Diego, CA). Statistical significance was determined by using two-way analysis of

variance (ANOVA) and the Student *t* test. Two-way ANOVA to compare the photoreceptor row counts and parameters of subretinal macrophage reactivity in C3 KO and WT animals with Tukey's post-hoc tests were performed to validate the comparisons. An unpaired Student *t* test was used to compare retinal GFAP responses (intensity and process lengths) in the C3 KO and WT mice. An alpha of less than 0.05 ($p<0.05$) was considered statistically significant.

RESULTS

Changes in photoreceptor death and GFAP levels in C3 KO mice after PD: The number of photoreceptor rows in the ONL was quantified to determine photoreceptor layer thickness after PD between the C3 KO and WT cohorts (Figure 1). The C3 KO and WT mice displayed fewer rows of photoreceptors in the superior retina, which is the focal region of damage in this model [27] after 7 days of PD ($p<0.05$, Figure 1A). In the C3 KO cohort, there was statistically significant rescue of photoreceptors in the superior retina compared to the wild-type controls ($p<0.05$, Figure 1A). Histologically, there was no perturbation in the retinal structure evident in either the WT or C3 KO mice (Figure 1B,C), as reported previously [16]. After 7 days of PD, there was severe thinning and disruption of the ONL in the WT mice. The thinning was not as apparent in the C3 KO cohort compared to the WT cohort (Figure 1D,E). The most pronounced disturbances in the WT retinas were observed in the central (about 500 µm eccentricity) and peripheral locations (about 1,000 µm eccentricity; Figure 1F,G). In the C3 KO retinas, there was some thinning of the ONL in the central location (about 500 µm eccentricity) following photo-oxidative damage, while the ONL was relatively intact in the peripheral retina (1,000 µm eccentricity; Figure 1H,I). In the WT cohort, there was also disruption of the RPE and the Bruch's membrane complex, while the outer retina featured large, amoeboid cells in the subretinal space (Figure 1J). Visually, there appeared to be no disruption of the RPE monolayer or Bruch's membrane in the C3 KO animals (Figure 1K).

In conjunction with these data, immunoreactivity for GFAP Müller cells was also assessed in the WT and C3 KO cohorts as a generalized marker of retinal stress [28]. GFAP immunoreactivity was not detectable in the Müller cell processes of either the dim-reared C3 KO or WT mice (Figure 2A,C), with no statistically significant difference detected in the GFAP fluorescence intensity between the two groups (Appendix 1, $p>0.05$). At 7 days of PD, GFAP immunoreactivity in Müller cells was readily apparent in the WT retinas, although it appeared less abundant in the C3 KO retinas (Figure 2B,D). The GFAP-positive processes extended from the inner retina into the outer nuclear layer in the WT retinas after photo-oxidative damage. These data were quantified through measurement of pixel intensity (Figure 2E) and the average length of the GFAP-positive Müller cells processes (Figure 2F), which were significantly lower in the C3 KO retinas compared to the WT retinas ($p<0.05$).

Modulation of macrophage activity in C3 KO mice following PD: The effect of C3 knockout on the migration and morphology of outer retinal macrophages was assessed across the time course of PD at 1, 3, 5, and 7 days (Figure 3A–F). Using immunolabeling for IBA1, the number of macrophages (the ONL and the subretinal space) in the WT mice increased progressively over the time course of PD from 3 days and reached a peak at 5 days (Figure 3G). In the C3 KO mice, however, the number of outer retinal macrophages was found to be reduced at 5 and 7 days compared to the WT retinas ($p<0.05$, Figure 3G). Morphological analysis of the microglia/macrophages situated within the ONL and the subretinal space was also conducted in the WT and C3 KO cohorts following PD (Figure 3H–J). Quantification of amoeboid versus ramified cells in this region demonstrated that an activated phenotype, characterized by the amoeboid morphology (Figure 3H, arrowheads), was less prevalent in the C3 KO mice after PD compared to the WT mice ($p<0.05$, Figure 3J). There was also trend in a higher number of ramified quiescent IBA1-positive cells in the C3 KO retinas (Figure 3I, arrowhead), although this trend was not statistically significant ($p>0.05$, Figure 3J).

Change in phagocytic markers and photoreceptor engulfment in outer retinal macrophages after PD: The distribution of phagocytosis-related markers in subretinal macrophages and their engulfment of photoreceptors were investigated to assess whether the morphological changes observed in the C3 KO mice (Figure 3J) were accompanied by changes in phagocytosis (Figure 4). Immunolabeling for CD68/macrosialin was used to interrogate phagocytosis and scavenger receptor activity in macrophages of the central nervous system (CNS; reviewed in [29]). After 7 days of PD, there was an abundance of IBA1-positive outer retinal macrophages that were immunoreactive for CD68 in the WT mice (Figure 4A,C), and these macrophages were more numerous in the superior retina where the focal point of injury is situated ($p<0.05$, Figure 4C). In contrast, there were far fewer ONL and subretinal macrophages that were CD68-positive in the C3 KO mice at the same time point ($p<0.05$, Figure 4B,C).

The IBA1-positive cells were colabeled with TUNEL to determine the change in the phagocytosis of photoreceptors by outer retinal macrophages in the WT and C3 KO cohorts (Figure 4D–I). These data were used to ascertain

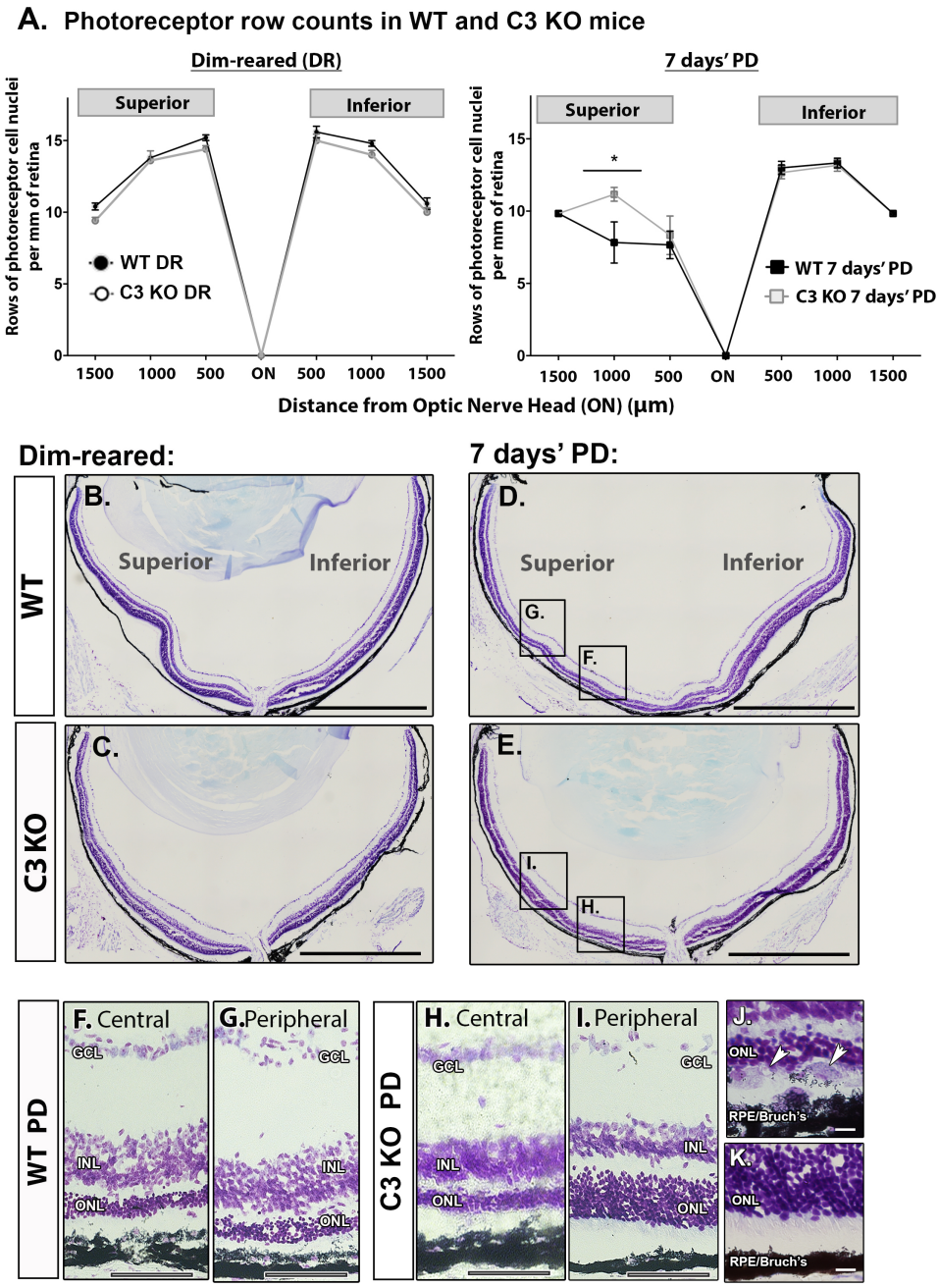

Figure 1. Changes in regional photoreceptor degeneration in C3 KO mice after 7 days of PD. **A**: There was no change in the average number of photoreceptors rows along the vertical meridian in C3 knockout (KO) versus wild-type (WT) mice retinas ($p>0.05$). Following PD, the C3 KO mice showed statistically significant preservation of the photoreceptor rows compared to the WT mice at 1,000 µm eccentricity from the ONL in the superior retina ($p<0.05$). **B, C**: Representative toluidine blue staining of retinal cross-sections showed no gross morphological difference between dim-reared WT (**B**) and C3 KO (**C**) groups. **D**–**I**: Representative staining of retina cross-sections after 7 days of PD indicate substantial deterioration the ONL in the WT mice (**D**), in the central (**F**, about 500 µm eccentricity) and peripheral (**G**, about 1,000 µm eccentricity) regions of the superior retina. In the C3 KO mice (**E**), representative images show severe ONL disruption mainly within the central region (**H**), while the peripheral region was more spared (**I**). **J**–**K**: Higher magnification examinations of WT mice retinas (**J**) following PD show the incursion of amoeboid cells in the subretinal space (arrowheads) and disruption of the RPE and Bruch's membrane complex which was scarcely documented in the C3 KO mice (**K**). Statistical significance was determined using two-way analysis of variance (ANOVA; $p<0.05$, $n = 6$ per experimental group). Scale bars represent 100 µm (**B**, **C**, **D**, and **E**), 50 µm (**F**, **G**, **H**, and **I**), and 10 µm (**J** and **K**). GCL, ganglion cell layer; INL, inner nuclear layer; ONL, outer nuclear layer; RPE, retinal pigment epithelium; PD, photo-oxidative damage; ON, optic nerve head.

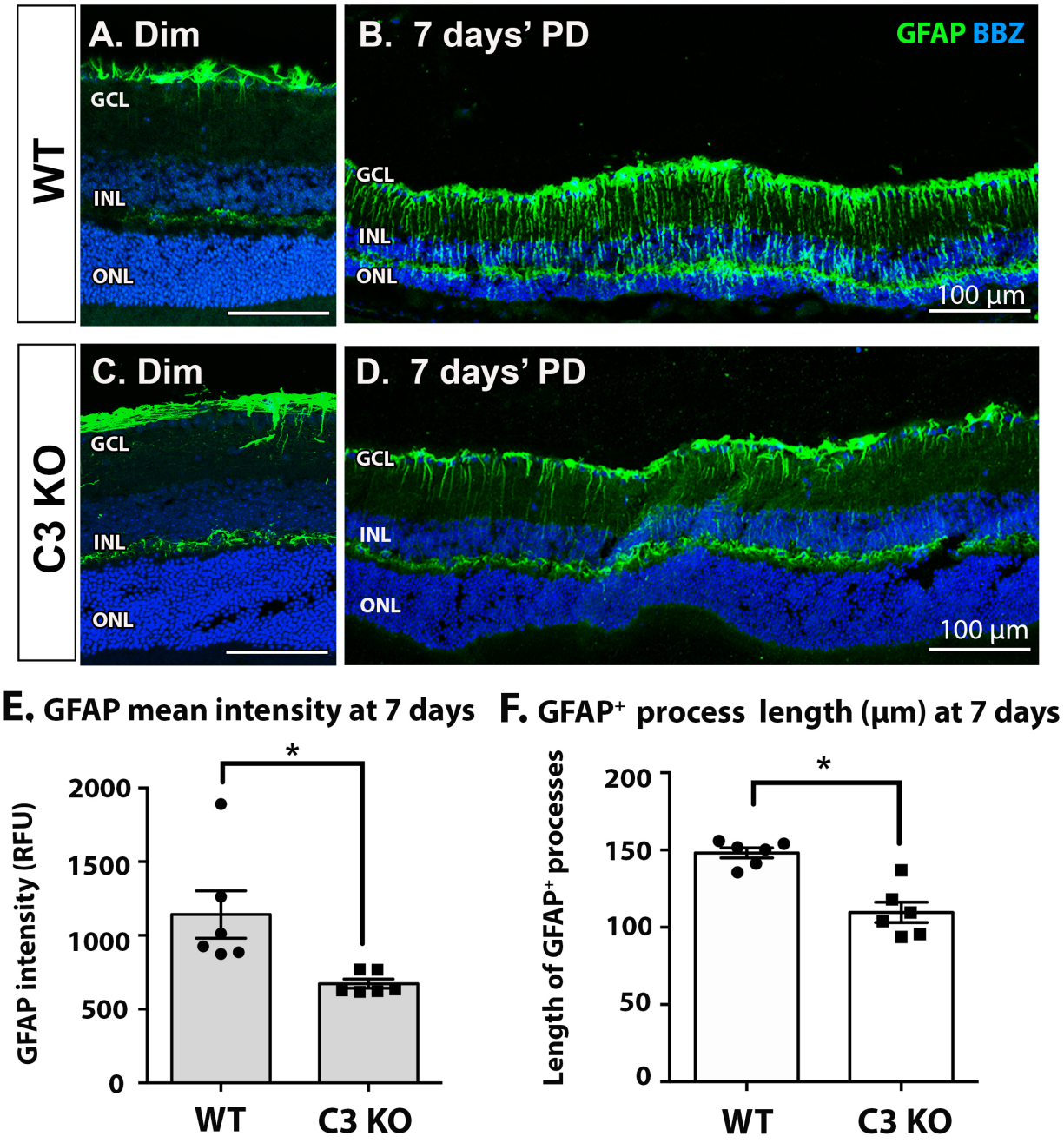

Figure 2. Change in immunoreactivity for GFAP in Müller glia of C3 KO mice after 7 days of PD. **A**–**D**: Representative retinal cross-sections that were fluorescently immunolabeled with GFAP (green) and counterstained with bisbenzamide (blue). There was limited immunofluorescence in the Müller glia from the dim-reared wild-type (WT; **A**) or C3 knockout (KO; **C**) mice. After PD, the WT retina sections exhibited strong immunofluorescence for GFAP in the Müller cell processes (**B**), which appeared less pronounced in the C3 KO retinas (**D**). **E**: GFAP mean fluorescence intensity was quantified in both cohorts at 7 days of PD, which showed a statistically significantly higher amount of immunoreactivity for the GFAP C3 KO mice compared to the GFAP WT mice ($p<0.05$). **F**: The average length of the GFAP-positive Müller cell processes was significantly lower in the C3 KO mice compared to the WT mice ($p<0.05$). Statistical significance was determined using the unpaired Student *t* test ($p<0.05$, n = 6 per group). Scale bars represent 100 µm (**B** and **D**) and 50 µm (**A** and **C**). GCL, ganglion cell layer; INL, inner nuclear layer; ONL, outer nuclear layer; RFU, relative fluorescence unit; RPE, retinal pigment epithelium; PD, photo-oxidative damage.

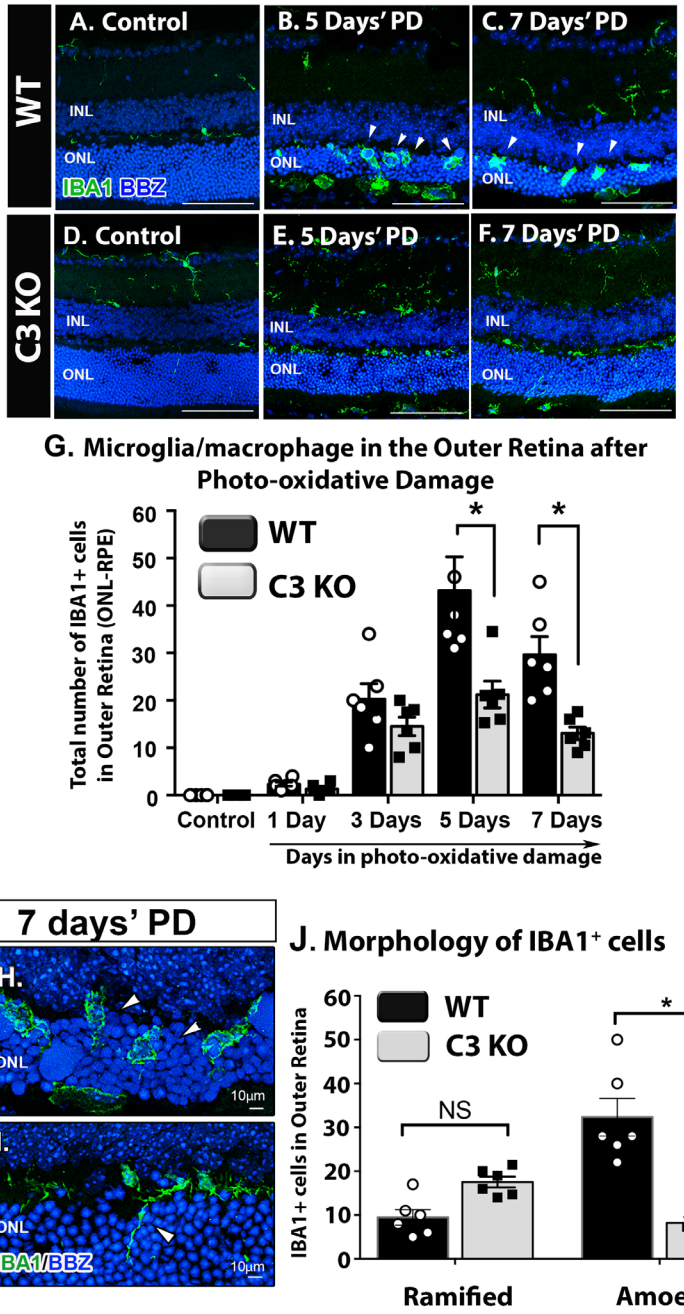

Figure 3. Incursion and morphological change in outer retinal macrophages from WT and C3 KO mice following a time course of PD. **A**–**F**: Representative retinal cross-sections fluorescently immunolabeled with IBA1 (green) and bisbenzamide (blue), in the 5- and 7-day PD groups. In the dim-reared retinas (**A**, **D**), IBA1-positive outer retinal macrophages were not present in either the wild-type (WT) or C3 knockout (KO) groups. After either 5 or 7 days of PD, a substantial incursion of macrophages was observed in the outer retina of the WT mice (**B**, **C**), which appeared less frequently in the C3 KO mice (**E**, **F**). **G**: Quantification of the average number of IBA1-positive outer retinal macrophages showed a statistically significant reduction in the C3 KO mice compared to the WT mice at the 5- and 7-day time points ($p<0.05$) but not at 1 or 3 days ($p>0.05$). **H**–**I**: Representative retinal cross-sections fluorescently immunolabeled with IBA1 (green) illustrate differences in the abundance of ameboid (**H**, arrowheads) and ramified (**I**, arrowhead) morphology in outer retinal macrophages in the WT and C3 KO mice after 7 days of PD. **J**: Quantification of ameboid and ramified IBA1-positive outer retinal macrophages at 7 days of PD revealed a substantial reduction in ameboid cells in the C3 KO mice compared to the WT mice ($p>0.05$). There was no statistically significant difference in the number of ramified IBA1-positive cells in the outer retina ($p>0.05$). Statistical significance was ascertained with two-way analysis of variance (ANOVA) with multiple comparisons (n = 6 per group; asterisks denote $p<0.05$). Scale bars represent 100 µm, unless indicated otherwise. INL, inner nuclear layer; ONL, outer nuclear layer; PD, photo-oxidative damage.

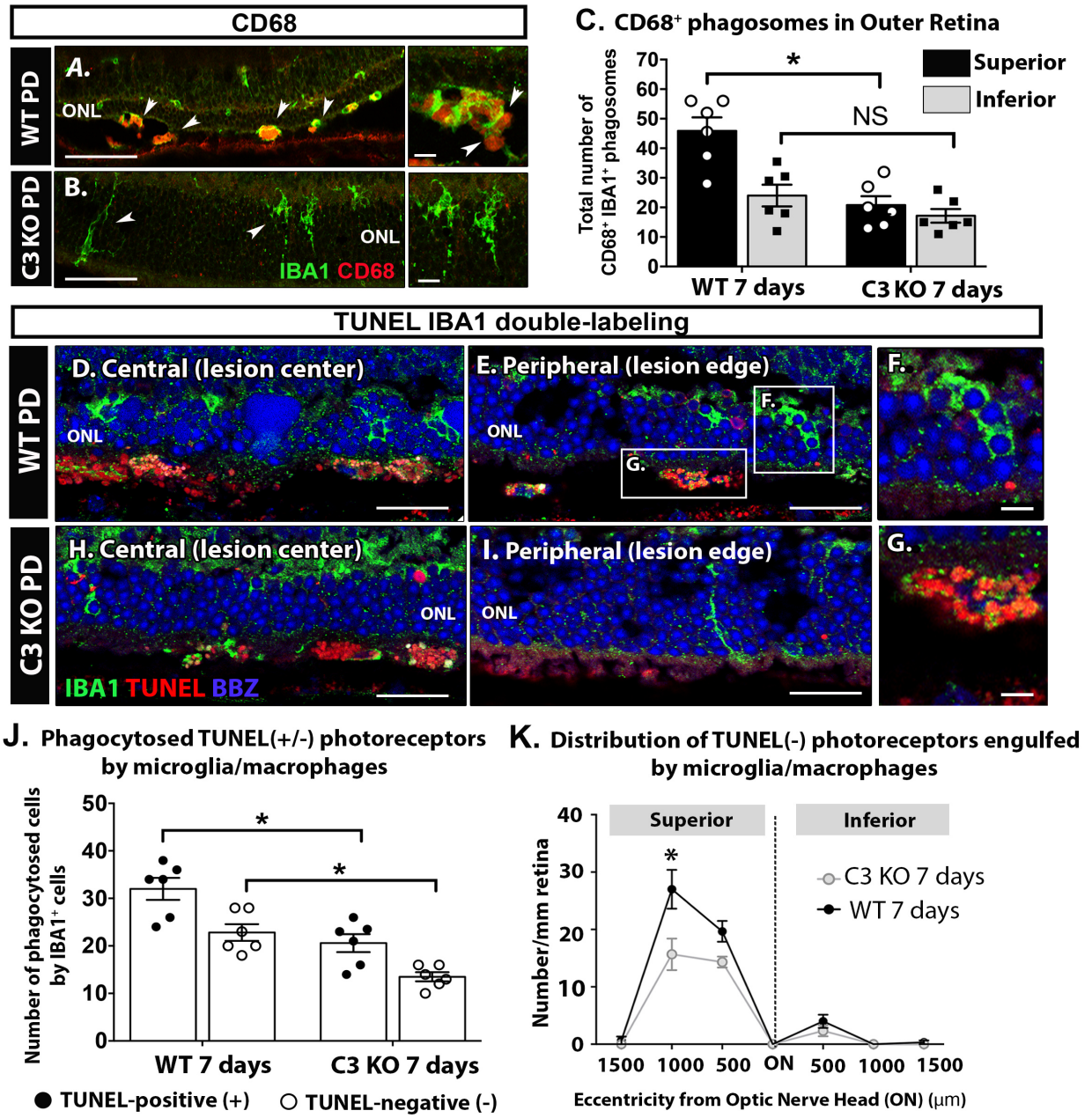

Figure 4. Change in phagocytosis-related properties by macrophages of the outer retina in C3 KO mice after 7 days of PD. **A**, **B**: Representative vertical sections immunolabeled for CD68/macrosialin (red) and IBA1 (green) to observe outer retinal macrophages in wild-type (WT) (**A**) and C3 knockout (KO) (**B**) mice after 7 days of PD. **C**: Quantification of CD68-positive/IBA1-positive cells in the outer retina on vertical sections indicates a statistically significant reduction in these cells in the C3 KO mice compared to the WT mice ($p<0.05$) following PD. **D**–**I**: Representative immunolabeling for terminal deoxynucleotidyl transferase dUTP nick end labeling (TUNEL) (red) and IBA1 (green) to observe changes in the engulfment of TUNEL-positive and -negative photoreceptors between the WT (**D**-G) and C3 KO mice (**H**-**I**). Both appeared to be similar in the WT (**D**) and C3 KO (**H**) groups at the central region of the superior retina which was the lesion center (500 μm eccentricity). In the C3 KO mice (**I**), the engulfment of TUNEL-positive and -negative photoreceptors were observed less frequently at the peripheral region of the superior retina which was the lesion edge (1,000 μm eccentricity) compared to the WT mice (**E**, **F**, and **G**). **J**: Quantification of TUNEL-positive/IBA1-positive (black) or TUNEL-negative/IBA1-positive (white) cells in the outer retina show that both groups are significantly smaller in the C3 KO cohort compared to the WT cohort ($p<0.05$) after 7 days of PD. **K**: Counts of TUNEL-negative/IBA1-positive cells in 500 μm increments across the vertical meridian reveal a peak in the engulfment of TUNEL-negative photoreceptors at 1,000 μm eccentricity in the WT mice, which is significantly lower in the C3 KO cohort ($p<0.05$). Statistical significance was determined via two-way analysis of variance (ANOVA) with multiple comparisons (n = 5–6 per group/time point; asterisks denote $p<0.05$). Scale bars represent 50 μm (**A**, **B**, **D**, **E**, **H**, **I**) and 10 μm (**F** and **G**). ONL, outer nuclear layer; ON, optic nerve head; PD, photo-oxidative damage.

not only the phagocytosis of apoptotic TUNEL-positive photoreceptors but also the phagocytosis of stressed but still viable TUNEL-negative photoreceptors, a process known as phagoptosis [30]. Double-labeling indicated that phagocytosis of TUNEL-positive photoreceptors by IBA1-positive cells was evident at the focal point of the lesion (Figure 4D, approximately 500 µm from the ON) and surrounding regions (Figure 4E,F,G, approximately 1000 µm from the ON) in the WT mice after 7 days of PD. In the C3 KO mice, this phagocytosis was restricted to the central retina, which was the center of the lesion at 7 days of PD (Figure 4H,I). When quantified, approximately 55% of the phagocytosed photoreceptors were TUNEL-positive in the WT retinas at 7 days of PD, while the remaining were TUNEL-negative (Figure 4J). In the C3 KO cohort, there were significantly fewer phagocytosed TUNEL-positive photoreceptors compared to the WT mice ($p<0.05$, Figure 4J). The number of phagocytosed viable photoreceptors (TUNEL-negative) was also lower in the C3 KO mice compared to the WT mice ($p<0.05$, Figure 4J). Stratification of TUNEL-negative/IBA1-positive cells in 500 µm increments across the vertical meridian indicated a peak in phagocytosis of TUNEL-negative photoreceptors at the lesion periphery or edge (1,000 µm eccentricity) in the WT mice ($p<0.05$, Figure 4K). In the C3 KO mice, however, the number of TUNEL-negative/IBA1-positive cells in this region (1,000 µm) was decreased by approximately one third ($p<0.05$, Figure 4K).

DISCUSSION

The present investigation sought to determine whether the neuroprotective phenotype of C3 ablation in PD is accompanied by changes in macrophage reactivity within the outer retina. The present study data show that C3 ablation suppressed photoreceptor death in a region-specific manner (in which more photoreceptors in the lesion margin were spared) and was associated with a reduction in the retinal stress marker GFAP. Furthermore, we observed spatiotemporal changes in the reactivity of outer retinal macrophages in C3-deficient mice following PD. First, there was a reduction in the number of macrophages in the ONL and the subretinal space in the C3 KO mice, and a reduction in those exhibiting an ameboid morphology compared to the WT mice. Second, outer retinal macrophages of the C3 KO mice were found to have reduced CD68-positive phagosomes compared to the WT mice. Finally, there was a decrease in the phagocytosis of TUNEL-positive and TUNEL-negative photoreceptors by macrophages in the C3 KO mice.

Previous investigations have shown that subretinal macrophages are predominantly mobilized resident microglia in PD [31]. The subretinal populations come from their niches in the inner retina, switching their functions toward proinflammatory as an attempt to protect the compromised RPE [32,33]. As PD recapitulates some events akin to the atrophic AMD [7,17], the present study data suggest that the central complement component C3 amplifies the subretinal macrophage activity and the progression of retinal degeneration. Targeting the local sources of C3 [34] can be potentially beneficial to mitigate the adverse effects of subretinal macrophages in the degenerating retina. Complement aids in furnishing macrophages with tools for recognizing and opsonizing cellular debris and apoptotic cells [35], and is associated with progressive retinal degeneration [13]. C3-dependent phagosome expression in macrophages contributes to neurodegeneration [36], including that observed in the retina [24]. In the present study, the lower number of phagosomes and ameboid macrophages coincides with the reduced phagocytosis following the ablation of C3, and with the mitigated progression of retinal atrophy.

Among the recent literature, the present study results suggest that the contribution of complement and macrophages to retinal degeneration is context-dependent, governed by the nature of the pathological cues encountered. In the *rd10* mouse model of retinitis pigmentosa (RP), the recent investigation by Silverman and colleagues indicated that complement aids in the clearance of accruing apoptotic photoreceptors by infiltrating macrophages/microglia. Although the ablation of C3 elicited dampened phagocytosis of photoreceptors in both investigations, the present data report a neuroprotective phenotype of C3 ablation in PD, rather than an overtly deleterious response as shown in RP. Moreover, genetic ablation of C3 accelerates photoreceptor degeneration, subretinal deposits, all of which link to impaired phagocytosis of RPE in aged C3 KO mice [37]. The reason for this discrepancy could lie in the larger extent of degeneration and maladaptive complement activity in the PD model, including activation of the proinflammatory alternative pathway of the cascade. In previous studies, ablation of alternative factors B and D has been shown to suppress local complement and photoreceptor death following PD [15,38]. Other maladaptive contributions of complement have been documented in loss of retinal ganglion cell synapses in the early and moderate stages of glaucoma in DBA/2J mice [39] and in an inducible rat model of glaucoma [40].

The reduction in phagocytosis of TUNEL-negative photoreceptors led us to speculate about a potential role for complement in promoting cell death through the phagoptosis of stressed but still-living photoreceptors. Phagoptosis arises from the expression of “eat me” signals of viable cells and

has been proposed as a contextual trigger for the destruction of neurons by activated microglia in the CNS (reviewed in [29,30]), including brain ischemia [41]. A maladaptive function of outer retinal macrophages in their elimination of neighboring viable rod photoreceptors has been reported in the *rd10* model [24]. Dampened phagocytosis of TUNEL-negative photoreceptors was also reported in the Silverman et al. study despite the deleterious effect of ablating C3, although a causative role of complement in this process is unclear. Nevertheless, the potential link between phagoptosis and complement in retinal degeneration certainly merits more in-depth investigation in future studies.

Conclusions: This investigation showed that ablation of C3 suppressed macrophage activity over the time course of PD, as evidenced by the altered morphology and cell density of macrophages in the outer retina. The ablation of C3 proved to be neuroprotective in PD despite the reduction in photoreceptor phagocytosis, suggesting an overtly maladaptive complement response in the given context. Although targeting complement could be useful in mitigating retinal atrophy [34], the results also indicate that targeting complement activity should be sought with caution to avoid impacting the phagocytic clearance.

APPENDIX 1. GFAP IMMUNOREACTIVITY IN DIM-REARED WT AND C3 KO RETINAS DISPLAY NO SIGNIFICANCE IN THE FLUORESCENCE INTENSITY BETWEEN THE GROUPS (P>0.05).

To access the data, click or select the words "Appendix 1."

ACKNOWLEDGMENTS

This study was supported by project grants from the National Health and Medical Research Council (APP1165599; APP1127705), Australian National University Translational Fellowship and Australian Government Research Training Program Scholarship.

REFERENCES

1. Merle NS, Church SE, Fremeaux-Bacchi V, Roumenina LT. Complement System Part I - Molecular Mechanisms of Activation and Regulation. Front Immunol 2015; 6:262-[PMID: 26082779].

2. Ricklin D, Hajishengallis G, Yang K, Lambris JD. Complement: a key system for immune surveillance and homeostasis. Nat Immunol 2010; 11:785-97. [PMID: 20720586].

3. Don H. Anderson, Monte J Radeke, Natasha B Gallo, Ethan A Chapin, Patrick T Johnson, Christy R Curletti, Lisa S Hancox, Jane Hu, Jessica N Ebright, Goldis Malek, Michael A Hauser, Catherine Bowes Rickman, Dean Bok, Gregory S Hageman, Lincoln V Johnson. The pivotal role of the complement system in aging and age-related macular degeneration: hypothesis re-visited. Prog Retin Eye Res 2010; 29:95-112. [PMID: 19961953].

4. Geerlings MJ, de Jong EK, den Hollander AI. The complement system in age-related macular degeneration: A review of rare genetic variants and implications for personalized treatment. Mol Immunol 2017; 84:65-76. [PMID: 27939104].

5. Ricklin D, Lambris JD. Therapeutic control of complement activation at the level of the central component C3. Immunobiology 2016; 221:740-6. [PMID: 26101137].

6. Carpanini SM, Torvell M, Morgan BP. Therapeutic Inhibition of the Complement System in Diseases of the Central Nervous System. Front Immunol 2019; 10:362-[PMID: 30886620].

7. Marc RE, Jones BW, Watt CB, Vazquez-Chona F, Vaughan DK, Organisciak DT. Extreme retinal remodeling triggered by light damage: implications for age related macular degeneration. Mol Vis 2008; 14:782-806. [PMID: 18483561].

8. Robert J Collier, Yu Wang, Sherry S Smith, Elizabeth Martin, Richard Ornberg, Kristina Rhoades, Carmelo Romano. Complement deposition and microglial activation in the outer retina in light-induced retinopathy: inhibition by a 5–HT1A agonist. Invest Ophthalmol Vis Sci 2011; 52:8108-16. [PMID: 21467172].

9. Rutar M, Natoli R, Kozulin P, Valter K, Gatenby P, Provis JM. Analysis of complement expression in light-induced retinal degeneration: synthesis and deposition of C3 by microglia/macrophages is associated with focal photoreceptor degeneration. Invest Ophthalmol Vis Sci 2011; 52:5347-58. [PMID: 21571681].

10. Peeters A, Magliano DJ, Stevens J, Duncan BB, Klein R, Wong TY. Changes in abdominal obesity and age-related macular degeneration: the Atherosclerosis Risk in Communities Study. Arch Ophthalmol 2008; 126:1554-60. [PMID: 19001224].

11. Ambati J, Atkinson JP, Gelfand BD. Immunology of age-related macular degeneration. Nat Rev Immunol 2013; 13:438-51. [PMID: 23702979].

12. Silverman SM, Wong WT. Microglia in the Retina: Roles in Development, Maturity, and Disease. Annu Rev Vis Sci 2018; 4:45-77. [PMID: 29852094].

13. Karlstetter M, Scholz R, Rutar M, Wong WT, Provis JM, Langmann T. Retinal microglia: Just bystander or target for therapy? Prog Retin Eye Res 2015; 45:30-57. [PMID: 25476242].

14. Rutar M, Valter K, Natoli R, Provis JM. Synthesis and Propagation of Complement C3 by Microglia/Monocytes in the Aging Retina. PLoS One 2014; 9:e93343-[PMID: 24705166].

15. Natoli R, Fernando N, Dahlenburg T, Jiao H, Aggio-Bruce R, Nigel L. Barnett, Juan Manuel Chao de la Barca, Guillaume Tcherkez, Pascal Reynier, Johnny Fang, Joshua A Chu-Tan, Krisztina Valter, Jan Provis, Matt Rutar. Obesity-induced metabolic disturbance drives oxidative stress and

complement activation in the retinal environment. Mol Vis 2018; 24:201-17. [PMID: 29527116].

16. Natoli R, Fernando N, Jiao H, Racic T, Madigan M, Nigel L. Barnett, Joshua A Chu-Tan, Krisztina Valter, Jan Provis, Matt Rutar. Retinal Macrophages Synthesize C3 and Activate Complement in AMD and in Models of Focal Retinal Degeneration. Invest Ophthalmol Vis Sci 2017; 58:2977-90. [PMID: 28605809].

17. Suzuki M, Tsujikawa M, Itabe H, Du Z-J, Xie P, Matsumura N, Fu X, Zhang R, Koh-hei S, Egashira K, Stanley L. Hazen, Motohiro Kamei. Chronic photo-oxidative stress and subsequent MCP-1 activation as causative factors for age-related macular degeneration. J Cell Sci 2012; 125:2407-15. [PMID: 22357958].

18. Silverman SM, Ma W, Wang X, Zhao L, Wong WT. C3- and CR3-dependent microglial clearance protects photoreceptors in retinitis pigmentosa. J Exp Med 2019; 216:1925-43. [PMID: 31209071].

19. Sennlaub F, Auvynet C, Calippe B, Lavalette S, Poupel L, Shulong J. Hu, Elisa Dominguez, Serge Camelo, Olivier Levy, Elodie Guyon, Noah Saederup, Israel F Charo, Nico Van Rooijen, Emeline Nandrot, Jean-Louis Bourges, Francine Behar-Cohen, José-Alain Sahel, Xavier Guillonneau, William Raoul, Christophe Combadiere. CCR2(+) monocytes infiltrate atrophic lesions in age-related macular disease and mediate photoreceptor degeneration in experimental subretinal inflammation in Cx3cr1 deficient mice. EMBO Mol Med 2013; 5:1775-93. [PMID: 24142887].

20. Ulrich FO. Luhmann, Scott Robbie, Peter M G Munro, Susie E Barker, Yanai Duran, Vy Luong, Frederick W Fitzke, James W B Bainbridge, Robin R Ali, Robert E MacLaren The drusenlike phenotype in aging Ccl2-knockout mice is caused by an accelerated accumulation of swollen autofluorescent subretinal macrophages. Invest Ophthalmol Vis Sci 2009; 50:5934-43. [PMID: 19578022].

21. Ng TF, Streilein JW. Light-induced migration of retinal microglia into the subretinal space. Invest Ophthalmol Vis Sci 2001; 42:3301-10. [PMID: 11726637].

22. . Fernando Cruz-Guilloty. Ali M Saeed, Jose J Echegaray, Stephanie Duffort, Asha Ballmick, Yaohong Tan, Michel Betancourt, Eduardo Viteri, Ghansham C Ramkhellawan, Eric Ewald, William Feuer, Deqiang Huang, Rong Wen, Li Hong, Hua Wang, James M Laird, Abdoulaye Sene, Rajendra S Apte, Robert G Salomon, Joe G Hollyfield, Victor L Perez Infiltration of proinflammatory m1 macrophages into the outer retina precedes damage in a mouse model of age-related macular degeneration. Int J Inflamm 2013; 2013:503725-.

23. Peng B, Xiao J, Wang K, So KF, Tipoe GL, Lin B. Suppression of microglial activation is neuroprotective in a mouse model of human retinitis pigmentosa. J Neurosci 2014; 34:8139-50. [PMID: 24920619].

24. Zhao L, Matthew K. Zabel, Xu Wang, Wenxin Ma, Parth Shah, Robert N Fariss, Haohua Qian, Christopher N Parkhurst, Wen-Biao Gan, Wai T Wong. Microglial phagocytosis of living photoreceptors contributes to inherited retinal degeneration. EMBO Mol Med 2015; 7:1179-97. [PMID: 26139610].

25. Schnabolk G, Coughlin B, Joseph K, Kunchithapautham K, Bandyopadhyay M. Elizabeth C O'Quinn, Tamara Nowling, Bärbel Rohrer. Local production of the alternative pathway component factor B is sufficient to promote laser-induced choroidal neovascularization. Invest Ophthalmol Vis Sci 2015; 56:1850-63. [PMID: 25593023].

26. Bosco A, Sarah R. Anderson, Kevin T Breen, Cesar O Romero, Michael R Steele, Vince A Chiodo, Sanford L Boye, William W Hauswirth, Stephen Tomlinson, Monica L Vetter. C3-Targeted Gene Therapy Restricts Onset and Progression of Neurodegeneration in Chronic Mouse Glaucoma. Mol Ther 2018; 26:2379-96. [PMID: 30217731].

27. Natoli R, Jiao H, Nigel L. Barnett, Nilisha Fernando, Krisztina Valter, Jan M Provis, Matt Rutar. A model of progressive photo-oxidative degeneration and inflammation in the pigmented C57BL/6J mouse retina. Exp Eye Res 2016; 147:114-27. [PMID: 27155143].

28. Yang Z, Wang KK. Glial fibrillary acidic protein: from intermediate filament assembly and gliosis to neurobiomarker. Trends Neurosci 2015; 38:364-74. [PMID: 25975510].

29. Fu R, Shen Q, Xu P, Luo JJ, Tang Y. Phagocytosis of microglia in the central nervous system diseases. Mol Neurobiol 2014; 49:1422-34. [PMID: 24395130].

30. Brown GC, Neher JJ. Eaten alive! Cell death by primary phagocytosis: 'phagoptosis'. Trends Biochem Sci 2012; 37:325-32. [PMID: 22682109].

31. Ma WX, Zhang YK, Gao C, Fariss RN, Tam J, Wong WT. Monocyte infiltration and proliferation reestablish myeloid cell homeostasis in the mouse retina following retinal pigment epithelial cell injury. Sci Rep-Uk. 2017;7.

32. O'Koren EG, Mathew R, Saban DR. Fate mapping reveals that microglia and recruited monocyte-derived macrophages are definitively distinguishable by phenotype in the retina. Sci Rep-Uk. 2016;6.

33. Emily G. O'Koren, Chen Yu, Mikael Klingeborn, Alicia Y W Wong, Cameron L Prigge, Rose Mathew, Joan Kalnitsky, Rasha A Msallam, Aymeric Silvin, Jeremy N Kay, Catherine Bowes Rickman, Vadim Y Arshavsky, Florent Ginhoux, Miriam Merad, Daniel R Saban. Microglial Function Is Distinct in Different Anatomical Locations during Retinal Homeostasis and Degeneration. Immunity 2019; 50:723-37. [PMID: 30850344].

34. David S. Liao, Federico V Grossi, Delphine El Mehdi, Monica R Gerber, David M Brown, Jeffrey S Heier, Charles C Wykoff, Lawrence J Singerman, Prema Abraham, Felix Grassmann, Peter Nuernberg, Bernhard H F Weber, Pascal Deschatelets, Robert Y Kim, Carol Y Chung, Ramiro M Ribeiro, Mohamed Hamdani, Philip J Rosenfeld, David S Boyer, Jason S Slakter, Cedric G Francois. C3 Inhibitor Pegcetacoplan for Geographic Atrophy Secondary to Age-Related Macular Degeneration: A Randomized Phase 2 Trial. Ophthalmology 2020; 127:186-95. [PMID: 31474439].

35. Stephan AH, Barres BA, Stevens B. The complement system: an unexpected role in synaptic pruning during development and disease. Annu Rev Neurosci 2012; 35:369-89. [PMID: 22715882].

36. Bodea L-G, Wang Y, Linnartz-Gerlach B, Kopatz J, Sinkkonen L, Musgrove R, Kaoma T, Muller A, Vallar L, Donato A Di M, Balling R, Neumann H. Neurodegeneration by Activation of the Microglial Complement-Phagosome Pathway. J Neurosci 2014; 34:8546-56. [PMID: 24948809].

37. Hoh Kam J, Lenassi E, Malik TH, Pickering MC, Jeffery G. Complement component C3 plays a critical role in protecting the aging retina in a murine model of age-related macular degeneration. Am J Pathol 2013; 183:480-92. [PMID: 23747511].

38. Rohrer B, Guo Y, Kunchithapautham K, Gilkeson GS. Eliminating complement factor D reduces photoreceptor susceptibility to light-induced damage. Invest Ophthalmol Vis Sci 2007; 48:5282-9. [PMID: 17962484].

39. Stevens B, Nicola J. Allen, Luis E Vazquez, Gareth R Howell, Karen S Christopherson, Navid Nouri, Kristina D Micheva, Adrienne K Mehalow, Andrew D Huberman, Benjamin Stafford, Alexander Sher, Alan M Litke, John D Lambris, Stephen J Smith, Simon W M John, Ben A Barres. The classical complement cascade mediates CNS synapse elimination. Cell 2007; 131:1164-78. [PMID: 18083105].

40. Pete A. Williams, James R Tribble, Keating W Pepper, Stephen D Cross, B Paul Morgan, James E Morgan, Simon W M John, Gareth R Howell. Inhibition of the classical pathway of the complement cascade prevents early dendritic and synaptic degeneration in glaucoma. Mol Neurodegener 2016; 11:26-[PMID: 27048300].

41. Neher JJ, Emmrich JV, Fricker M, Mander PK, Thery C, Brown GC. Phagocytosis executes delayed neuronal death after focal brain ischemia. Proc Natl Acad Sci USA 2013; 110:E4098-107. [PMID: 24101459].

Articles are provided courtesy of Emory University and the Zhongshan Ophthalmic Center, Sun Yat-sen University, P.R. China. The print version of this article was created on 10 October 2020. This reflects all typographical corrections and errata to the article through that date. Details of any changes may be found in the online version of the article.